Anal. Chem. **2002,** *74,* 3297−3303

Unusual Response in Mediated Biosensors with an Oxidase/Peroxidase Bienzyme System

Ryuhei Matsumoto, Manabu Mochizuki, Kenji Kano,* and Tokuji Ikeda

Division of Applied Life Sciences, Graduate School of Agriculture, Kyoto University, Sakyo-ku, Kyoto 606-8502, Japan

Mediated biosensors consisting of an oxidase and peroxidase (POx) have attracted increasing attention because of their wide applicability. However, since most of oxidases utilize artificial electron acceptors in place of dioxygen, the competition between O_2 and the electron acceptor in the mediated sensors is anticipated. This has been evidenced with a glucose oxidase (GOx)- and POx-coentrapped and ferrocene-embedded carbon paste electrode, which exhibits peak-shaped current−time curves at increased concentrations of glucose and also gives a peak-shaped calibration curve. Digital simulation has been applied to clarify the cause of such unusual responses, by taking into account the ping-pong enzyme kinetics on two- and three-substrate models for POx and GOx, respectively. The simulation has well reproduced such unusual responses and has clearly revealed that the depletion of O_2 in the enzyme layer is the most important factor responsible for such unusual responses. To overcome such a drawback of oxidase/POx bienzyme sensors, it is expected to be essential to decrease the rate of the oxidase reaction. In contrast, increase in the POx activity is useful to improve the sensitivity. According to the simulation-based expectation, the GOx and POx concentrations in the bienzyme sensor are adjusted to exhibit normal behavior with high sensitivity.

Peroxidase (POx)-catalyzed mediated bioelectrochemical sensors for hydrogen peroxide detection have attracted increasing attention.[1−6] The electrochemical detection of H_2O_2 is based on the reduction of oxidized mediator generated by POx-catalyzed reduction of H_2O_2 into H_2O, in which iron[3,4,7−10] or osmium complexes[2] or phenotiazin derivatives[5] may be utilized as mediators. Therefore, H_2O_2 detection can be performed around 0 mV (vs Ag/AgCl), where the background current is quickly stabilized to a very small value. This allows highly sensitive detection.[6,8,11] The POx-based H_2O_2 detection system has been coupled with several oxidase reactions to construct a variety of biosensors for biologically related compounds.[12−20]

However, most oxidases utilize several artificial (or nonphysiological) electron acceptors other than dioxygen.[21] This reaction will be called dehydrogenase activity in this paper, while the term "oxidase activity" is restrictively used for the reaction with O_2. Therefore, such bienzyme systems have inherently a possibility of suffering from interference due to the competition between O_2 (a natural electron acceptor in the oxidase activity) and an oxidized mediator (an artificial electron acceptor in the dehydrogenase activity).[8,12,22] Scheme 1 illustrates such reactions for a case involving glucose oxidase (GOx) and ferrocene (Fc) as an oxidase and a mediator, respectively. Ferricenium cation (Fc^+) generated in the POx reaction may participate in the GOx-catalyzed glucose dehydrogenase reaction, which causes a decrease in the electrochemical signal (the reduction current of Fc^+).

In this work, we constructed a GOx/POx-coentrapped and Fc-embedded carbon paste electrode. The electrode exhibited unusual current−time response due to the competition of oxidase and dehydrogenase activity of GOx, and the steady-state current did not exhibit a one-to-one relation against the glucose concentration. Such behavior leads to erroneous determination of glucose. To understand this phenomenon clearly, we applied digital simulation based on Michaelis−Menten-type enzyme kinetics to

* Corresponding author: (fax) +81-75-753-6393; (e-mail) kkano@kais.kyoto-u.ac.jp.

(1) Ruzgas, T.; Csöregi, E.; Emnéus, J.; Gorton, L.; Marko-Varga, G. *Anal. Chim. Acta* **1996**, *330*, 123−138.
(2) Vreeke, M. S.; Yong, K. T.; Heller, A. *Anal. Chem.* **1995**, *67*, 4247−4249.
(3) Sakai, H.; Baba, R.; Hashimoto, K.; Fujishima, A.; Heller, A. *J. Phys. Chem.* **1995**, *99*, 11896−11900.
(4) Wang, J.; Liu, J.; Cepra, G. *Anal. Chem.* **1997**, *69*, 3124−3127.
(5) Razola, S. S.; Aktas, E.; Vire, J. C.; Kauffmann, J. M. *Analyst* **1999**, *125*, 79−85.
(6) Yamamoto, K.; Ohgaru, T.; Torimura, M.; Kinoshita, H.; Kano, K.; Ikeda, T. *Anal. Chim. Acta* **2000**, *406*, 201−207.
(7) Ikeda, T.; Shiraishi, T.; Senda, M. *Agric. Biol. Chem.* **1988**, *52*, 3187−3188.
(8) Kinoshita, H.; Torimura, M.; Kano, K.; Ikeda, T. *Electroanalysis* **1997**, *9*, 1234−1238.
(9) Wang, J.; Reviejo, A. J.; Angnes, L. *Electroanalysis* **1993**, *5*, 575−579.
(10) Sánchez, P. D.; Ordieres, A. J. M.; García, A. C.; Blanco, P. T. *Electroanalysis* **1991**, *3*, 281−285.
(11) Yang, L.; Janle, E.; Huang, T.; Gitzen, J.; T. Kissinger, P. T.; Vreeke M.; Heller, A. *Anal. Chem.* **1995**, *67*, 1326−1331.
(12) Kenausis, G.; Cheng, Q.; Heller, A. *Anal. Chem.* **1997**, *69*, 1054−1060.
(13) Maidan, R.; Heller, A. *Anal. Chem.* **1992**, *64*, 2889−2896.
(14) Ohara, T. J.; Vreeke, M. S.; Battaglini, F.; Heller, A. *Electroanalysis* **1993**, *5*, 825−831.
(15) Vijayakumar, A. R.; Csöregi, E.; Heller, A. *Anal. Chim. Acta* **1996**, *327*, 223−234.
(16) Kacaniklic, V.; Johansson, K.; Marko-Varga, G.; Gorton, L.; Jönsson-Pettersson, G.; Csöregi, E. *Electroanalysis* **1994**, *6*, 381−390.
(17) Belay, A.; Collins, A.; Ruzgas, T.; Kissinger, P. T.; Gorton, L.; Csöregi, E. *J. Pharm. Biomed. Anal.* **1999**, *19*, 93−105.
(18) Csöregi, E.; Gortson, L.; Marko-Varga, G. *Electroanalysis* **1994**, *6*, 925−933.
(19) Gorton, L.; Jönsson-Pettersson, G.; Csöregi, E.; Johansson, K.; Domínguez, E.; Marko-Varga, G. *Analyst* **1992**, *17*, 1235−1241.
(20) del Cello, M. A.; Cayuela, G.; Reviejo, A. J.; Pingarrón, J. M.; Wang, J. *Electroanalysis* **1997**, *9*, 1113−1119.
(21) Kano, K.; Ikeda, T. *Anal. Sci.* **2000**, *16*, 1013−1021.
(22) Kinoshita, H.; Torimura, M.; Yamamoto, K.; Kano, K.; Ikeda, T. *J. Electroanal. Chem.* **1999**, *478*, 33−39.

10.1021/ac015684n CCC: $22.00
Published on Web 05/25/2002

Scheme 1. Reactions Scheme of GOx/POx Bienzyme Sensor Containing Fc as a Mediator

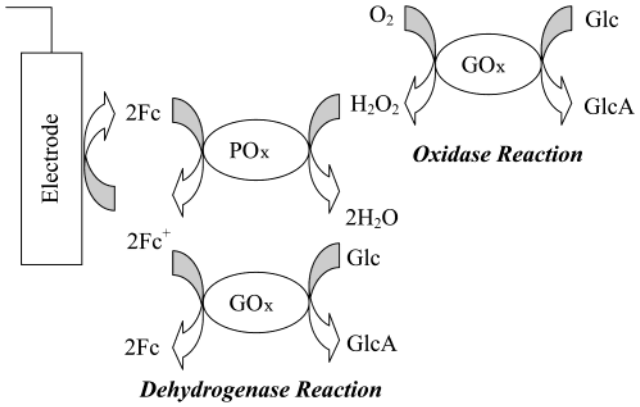

get the current response and the concentration profiles of the reactants in the enzyme layer on the electrode surface. The calculation revealed that O_2 depletion in the enzyme layer is the most important factor to cause unusual current responses. Several approaches to overcoming such an unusual current response are described.

EXPERIMENTAL SECTION

Chemicals. GOx (EC 1.1.3.4; 348 units mg^{-1}) and POx (EC 1.11.1.7; 100 units mg^{-1}) were purchased from Oriental and Toyobo, respectively. Polycarbonate membranes (pore size 0.8 μm, thickness 9 μm) were purchased from Advantec Co. Ltd. All other chemicals were of reagent grade quality.

Preparation of Modified Electrode. The carbon paste electrode (002210) was purchased from Bioanalytical Systems (BAS). Fc, paraffin oil, and graphite powder (Nippon Kokuen Co.) were thoroughly mixed at the ratio of 0.2 g, 150 μL, and 1.0 g, respectively. The mixture was tightly packed into the well of the electrode, and the surface of the electrode was smoothed on a weigh paper with pressure. An aliquot of GOx (1 mg mL^{-1}), POx (1 mg mL^{-1}), and bovine serum albumin (BSA, 1 mg mL^{-1}) solutions and 6 μL of 0.1% glutaraldehyde in ethanol solution were dropped in turn on the electrode surface and well mixed with the tip of a syringe. The solvent was evaporated for ~2 h at room temperature. This electrode was covered with a polycarbonate membrane, which was fixed tightly with an O-ring. The electrode was stored in 0.1 M phosphate buffer (pH 7.0) at 4 °C when it was not in use.

Electrochemical Measurements. All measurements were performed with a BAS electrochemical analyzer CV-50W using an Ag|AgCl|saturated KCl reference electrode and a Pt disk counter electrode at 25 °C. The basal solution used was usually 0.1 M phosphate buffer (pH 7.0, ionic strength 0.1). Constant-potential amperometric determination of glucose was done at 0 mV (vs Ag|AgCl|saturated KCl) under stirring (500 rpm) with a magnetic bar without deaeration. The steady-state current became independent of the stirring rate at and above 500 rpm, where the mass transfer would be controlled by the permeability of the membrane, and then the concentration depletion outside of the membrane would be neglected.[23]

(23) Ikeda, T.; Kurosaki, T.; Takayama, K.; Kano, K. *Anal. Chem.* **1996**, *68*, 192−198.

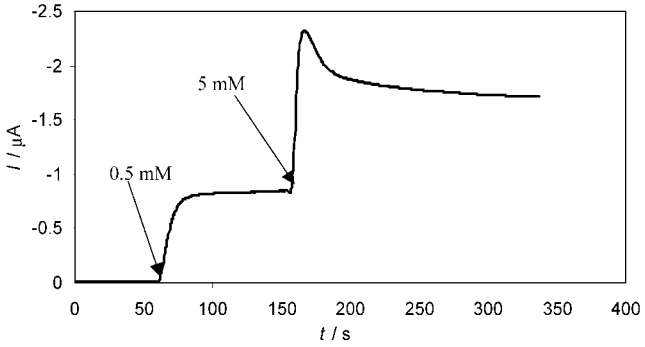

Figure 1. Amperometric response for successive injection of 0.5 and 5 mM glucose at a GOx/POx-coentrapped Fc-embedded carbon paste electrode at 0 mV (vs Ag|AgCl|saturated KCl) under stirring in 0.1 M phosphate buffer (pH 7.0). The bienzyme sensor contained 0.90 unit of GOx, 0.22 unit of POx, and 2 ng of BSA.

To determine the enzyme kinetic parameters of POx, ferrocenedicarboxylic acid ($Fc(COOH)_2$) was used as an electron donor. The initial rate of the consumption of $Fc(COOH)_2$ due to the POx reaction was determined as a function of the H_2O_2 concentration by amperometry with a rotating disk carbon electrode at 0.8 V and at 25 °C. The initial concentration of $Fc(COOH)_2$ was set at 8 mM.

Cyclic voltammograms were obtained with a bare glassy carbon electrode for determining the enzyme kinetics of dehydrogenase activity of GOx[21] under anaerobic and quiet conditions using $Fc(COOH)_2$ as a mediator at a scan rate of 10 mV s^{-1}.

Spectroscopy. UV−visible spectroscopy and spectrophotometry were performed with a Shimadzu Multi-Spec 1500. The concentrations of POx and GOx were, respectively, determined using the absorption coefficient of 102 000 M^{-1} cm^{-1} at 403 nm[24] and 18 240 M^{-1} cm^{-1} at 460 nm.[25]

RESULTS AND DISCUSSIONS

Current Response at a GOx/POx Bienzyme Sensor. Figure 1 shows an example of the amperometric response observed with a GOx/POx bienzyme sensor for the successive injection of glucose sample under stirring. When a glucose sample was injected at low concentrations (e.g., 0.5 mM), the reduction current increased immediately just after the injection and reached a steady-state maximum value. This is normal behavior. However, at higher glucose concentrations (e.g., 5.0 mM), the current−time curve exhibited a peak-shaped response after the sample injection and then reached a steady-state value.

As shown in Figure 2, the steady-state current increased linearly at low concentrations of glucose, where the current−time curve exhibited a normal response. With an increase in the glucose concentration, however, the steady-state current went down and reached a certain value, resulting in a peak-shaped calibration curve. Such behavior leads to serious error in the measurements of glucose, since the calibration curve no longer has a one-to-one relation against the glucose concentration.

The concentration of H_2O_2 in the enzyme layer would be much lower than the dissolved O_2 concentration (0.25 mM) and then would not be high enough to inhibit enzyme reactions.[26] Therefore, such unusual or undesired response of the current observed

(24) Keilin, D.; Hartree, E. F. *Biochem. J.* **1951**, *49*, 88−104.
(25) *Biochemical Data Book*; Japan Biochemical Society, Tokyo Kagaku Dojin: Tokyo, 1979; Vol. 1, p 105 (in Japanese).

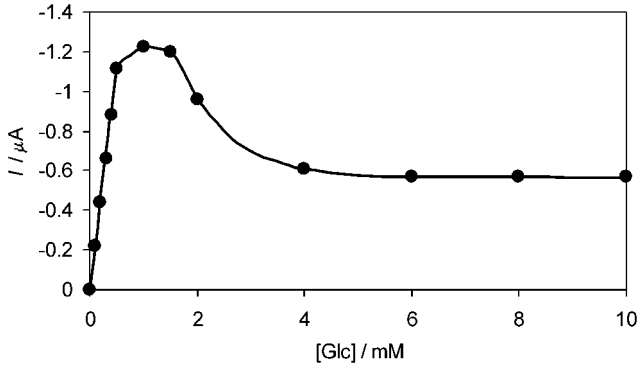

Figure 2. Steady-state current as a function of the glucose concentration obtained with a GOx/POx-coentrapped Fc-embedded carbon paste electrode, which contained 3.5 unit of GOx, 0.2 unit of POx, and 6 ng of BSA. The current was recorded at 0 mV (vs Ag|AgCl|saturated KCl) under stirring in 0.1 M phosphate buffer (pH 7.0).

at high concentrations of glucose can be reasonably ascribed to the competition of O_2 with Fc^+ for the glucose oxidation catalyzed by GOx. Although theoretical treatments on monoenzyme-type mediated biosensors have been published under steady-state conditions,[27,28] such theoretical treatment would be much more difficult for the bienzyme-type sensor system. In addition, it is important to describe not only steady-state response but also transient behavior. For this purpose, we try to get the concentration profile of reactants in the enzyme layer as a function of the time and length and discuss the behavior.

Steady-State Reaction of POx. The mechanism of POx reaction has been intensively examined.[26,29] The resting state of POx is oxidized with H_2O_2 to compound I (two-electron oxidized form), which is successively rereduced by one-electron-donating cosubstrate (M_{red}) via an intermediate compound II. Enzyme kinetics involving enzyme−substrate complexes has been reported.[26] To reduce the parameters, however, we assume that the reaction follows a simple ping-pong mechanism[30] as in the case of most of oxidoreductases with an enzyme-bound redox center and that the one-electron reduction of compound II with M_{red} is not the rate-determining step, as shown by

$$\mathrm{POx_{(rest)}} + \mathrm{H_2O_2} \underset{k_{-1}}{\overset{k_1}{\rightleftharpoons}} \mathrm{POx{-}H_2O_2} \xrightarrow{k_2} \mathrm{POx_{(compound\ I)}} + 2\mathrm{H_2O} \quad (1)$$

$$\mathrm{POx_{(compound\ I)}} + \mathrm{M_{red}} \underset{k_{-3}}{\overset{k_3}{\rightleftharpoons}} \mathrm{POx{-}M_{red}} \xrightarrow{k_4} \mathrm{POx_{(compound\ II)}} + \mathrm{M_{ox}} \quad (2a)$$

$$\mathrm{POx_{(compound\ II)}} + \mathrm{M_{red}} \xrightarrow{\text{fast}} \mathrm{POx_{(rest)}} + \mathrm{M_{ox}} \quad (2b)$$

where POx−H_2O_2 and POx−Fc denote the corresponding enzyme−substrate complexes (In this scheme and in the following discussion, protons involved in the enzyme reactions are eliminated for the sake of simplicity). Thus, the kinetics of the steady-state POx reactio (= v_{POx}) is given for the consumption of H_2O_2 by[30]

$$v_{POx} = \frac{V_{max}^{POx}}{1 + \dfrac{K_M^{POx}}{[M_{red}]} + \dfrac{K_S^{POx}}{[H_2O_2]}} \quad (3)$$

while the rate of M_{red} consumption is given by $2v_{POx}$. Here V_{max}^{POx} (= k_{cat}^{POx}[POx]) is the maximum velocity of the POx reaction, where k_{cat}^{POx} (= $k_2k_4/(k_2 + k_4)$) and [POx] are the catalytic constant and the POx concentration, respectively. K_M^{POx} (= $k_2(k_{-3} + k_4)/k_3(k_2 + k_4)$) and K_S^{POx} (= $k_4(k_{-1} + k_2)/k_1(k_2 + k_4)$) are the Michaelis constant of POx for M_{red} and H_2O_2, respectively.

In our case, it may be assumed that the concentration of Fc dissolved in the enzyme layer from the carbon paste electrode ([Fc]) is sufficiently larger than K_M^{POx}.[31,32] Therefore, eq 3 is reduced to

$$v_{POx} = \frac{V_{max}^{POx}}{1 + \dfrac{K_S^{POx}}{[H_2O_2]}} \quad (4)$$

The steady-state kinetic parameters of POx was determined with a rotating disk electrode using $Fc(COOH)_2$ in place of Fc, because of the low solubility of Fc in aqueous solution. The kinetic parameters were evaluated as $k_{cat}^{POx} = 14\ s^{-1}$ and $K_S^{POx} = 0.2$ mM on the basis of eq 4.

Enzyme Kinetics of GOx with Two Electron Acceptors. The electrochemical response of a conventional GOx-based glucose sensor was reported by considering the competitive activities of oxidase and dehydrogenase reactions using an approximate equation for the steady-state GOx reaction with two different electron acceptors.[33] However, GOx (oxidase reaction) is known to proceed in a ping-pong mechanism:

$$\mathrm{GOx_{(ox)}} + \mathrm{Glc} \underset{k_{-5}}{\overset{k_5}{\rightleftharpoons}} \mathrm{GOx{-}Glc} \xrightarrow{k_6} \mathrm{GOx_{(red)}} + \mathrm{GlcA} \quad (5)$$

$$\mathrm{GOx_{(red)}} + \mathrm{O_2} \underset{k_{-7}}{\overset{k_7}{\rightleftharpoons}} \mathrm{GOx{-}O_2} \xrightarrow{k_8} \mathrm{GOx_{(ox)}} + \mathrm{H_2O_2} \quad (6)$$

Glc and GlcA denote glucose and gluconic acid, respectively. GOx−Glc and GOx−O_2 are the corresponding enzyme−substrate complexes. The reoxidation of $GOx_{(red)}$ with an artificial one-electron acceptor (M_{ox}) has been investigated,[34] where a ping-pong-like mechanism is evidenced, but the precise enzyme kinetics is complicated. Therefore, we assume again that the one-

(26) Dequaire, M.; Limoges, B.; Moiroux, J.; Savéant, J.-M. *J. Am. Chem. Soc.* **2002**, *124*, 240−253.
(27) Bartlett, P. N.; Pratt, K. F. E. *J. Electroanal. Chem.* **1995**, *397*, 61−78.
(28) Ikeda, T.; Miki, K.; Senda, M. *Anal. Sci.* **1988**, *4*, 133−138.
(29) Rodríguez-López, J. N.; Lowe, D. J.; Hernández-Ruiz, J.; Hiner, A. N. P.; Carcía-Cánovas, F.; Thornely, R. N. F. *J. Am. Chem. Soc.* **2001**, *123*, 11838−11847.
(30) Segel, I. H. *Enzyme Kinetics*; Wiley: New York, 1975; Chapter 7.
(31) K_M^{POx} for Fc was not determined. Although K_M^{POx} for hydroquinone (= 2.8 mM[32]) is larger than the initial concentration of Fc assumed here, eq 4 is formally valid as long as the Fc concentration is practically constant in the enzyme layer.
(32) Ohgaru, T.; Tatsumi, H.; Kano, K.; Ikeda, T. *J. Electroanal. Chem.* **2001**, *496*, 37−43.
(33) Martens, N.; Hall, E. A. H. *Anal. Chem.* **1994**, *66*, 2763−2770.
(34) Bourdillon, V.; Demaille, V.; Moiroux, J.; Savéant, J.-M. *J. Am. Chem. Soc.* **1993**, *115*, 2−10.

electron oxidation of $GOx_{(red)}$ follows a simple ping-pong mechanism to yield its flavosemiquinone intermediate ($GOx_{(sem)}$) and that the succeeding one-electron oxidation of $GOx_{(sem)}$ with M_{ox} is not a rate-determining step.

$$GOx_{(red)} + M_{ox} \underset{k_{-9}}{\overset{k_9}{\rightleftharpoons}} GOx{-}M_{ox} \xrightarrow{k_{10}} GOx_{(sem)} + M_{red} \quad (7a)$$

$$GOx_{(sem)} + M_{ox} \xrightarrow{\text{fast}} GOx_{(ox)} + M_{red} \quad (7b)$$

Enzymatic reactions 6 and 7 are oxidase and dehydrogenase reactions, respectively. By applying the steady-state approximation to each species of GOx in the reactions as well as by using a mass balance equation for GOx, one can derive the following equations for the steady-state enzyme kinetics of the oxidase ($= v_{OX} = d[H_2O_2]/dt$) and dehydrogenase ($= v_{DH} = d[M_{red}]/2dt$) reactions of GOx in solution.

$$v_{OX} = \frac{\dfrac{[O_2]}{K_M^{OX}} V_{max}^{OX}}{1 + \dfrac{[O_2]}{K_M^{OX}} + \dfrac{[M_{ox}]}{K_M^{DH}} + \left(\dfrac{K_S^{OX}}{K_M^{OX}}[O_2] + \dfrac{K_S^{DH}}{K_M^{DH}}[M_{ox}]\right)/\{[Glc]\}} \quad (8)$$

$$v_{DH} = \frac{\dfrac{[M_{ox}]}{K_M^{DH}} V_{max}^{DH}}{1 + \dfrac{[O_2]}{K_M^{OX}} + \dfrac{[M_{ox}]}{K_M^{DH}} + \left(\dfrac{K_S^{OX}}{K_M^{OX}}[O_2] + \dfrac{K_S^{DH}}{K_M^{DH}}[M_{ox}]\right)/[Glc]} \quad (9)$$

where $V_{max}^{OX}(= k_{cat}^{OX}[GOx])$ and $V_{max}^{DH}(= k_{cat}^{DH}[GOx])$ are the maximum velocity of the oxidase and dehydrogenase reactions of GOx, [GOx] being the concentration of GOx. In the oxidase reaction, k_{cat}^{OX} $(= k_6k_8/(k_6 + k_8))$ is the catalytic constant, and K_S^{OX} $(= k_8(k_{-5} + k_6)/k_5(k_6 + k_8))$ and K_M^{OX} $(= k_6(k_{-7} + k_8)/k_7(k_6 + k_8))$ are the Michaelis constant for glucose and O_2, respectively. On the other hand, in the dehydrogenase reaction, k_{cat}^{DH} $(= k_6k_{10}/(k_6 + k_{10}))$ is the catalytic constant, and K_S^{DH} $(= k_{10}(k_{-5} + k_6)/k_5(k_6 + k_{10}))$ and K_M^{DH} $(= k_6(k_{-9} + k_{10})/k_9(k_6 + k_{10}))$ are the Michaelis constant for glucose and M_{ox}, respectively.

The enzymatic parameters for the oxidase reaction are available in the literature[35] ($k_{cat}^{OX} = 340\ s^{-1}$, $K_M^{OX} = 0.2$ mM, and $K_S^{OX} = 26$ mM). The bimolecular rate constant between $GOx_{(red)}$ and O_2 is 1.7×10^6 M s^{-1} $(= k_{cat}^{OX}/K_M^{OX})$. The dehydrogenase activity-related parameters k_{cat}^{DH} and K_M^{DH} were evaluated with cyclic voltammetry from the steady-state catalytic limiting current (I_{lim}) of mediated bioelectrocatalysis[32] using $Fc(COOH)_2$ as a mediator in place of Fc. The I_{lim} can be expressed as a function of the mediator concentration [M] by[32,36]

$$I_{lim} = \frac{n_M FA[M]}{1 + f_c}\sqrt{\frac{(n_S/n_M)D_M k_{cat}^{DH}[GOx]}{K_M^{DH} + [M]/2}} \quad (10)$$

where n_S and n_M are the number of electrons of the substrate (glucose) and the mediator (Fc), respectively ($n_S = 2$, $n_M = 1$) and F and A have their usual meanings. The parameter f_c is a digital simulation-based correction factor given by[32]

$$f_c = \frac{[M]/K_M^{DH}}{0.85([M]/K_M^{DH})^2 + 11.4([M]/K_M^{DH}) + 17.9} \quad (11)$$

The diffusion coefficient D_M (or $A(D_M)^{1/2}$) value was evaluated by potential-step chronoamperometry of $Fc(COOH)_2$ solution in the absence of glucose and GOx. The kinetic parameters k_{cat}^{DH} and K_M^{DH} were evaluated as $k_{cat}^{DH} = 350\ s^{-1}$ and $K_M^{DH} = 3.17$ mM by nonlinear least-squares analysis of I_{lim} versus $[Fc(COOH)_2]$ plots. The bimolecular rate constant between $GOx_{(red)}$ and $Fc^+(COOH)_2$ $(= k_{cat}^{DH}/K_M^{DH} = 1.1 \times 10^5\ M\ s^{-1})$ is 1 order smaller that that for O_2, but V_{max}^{DH} is slightly larger than V_{max}^{OX} $(V_{max}^{DH}/V_{max}^{OX} = k_{cat}^{DH}/k_{cat}^{OX} = 1.03)$. The K_S^{DH} value was calculated to be 27 mM by taking into account the relation $k_{cat}^{OX}/K_S^{OX} = k_{cat}^{DH}/K_S^{DH} = k_5k_6/(k_{-5} + k_6)$. The k_{cat}^{DH} and K_S^{DH}values are comparable with those reported in the literature ($497\ s^{-1}$, 29 mM).[37] The enzymatic parameters described above were used in the following calculations.

Digital Simulation. The explicit point method was used to obtain the concentration profile and I_{sim}.[38] The initial concentrations of Fc, Fc^+, O_2, H_2O_2, and glucose were assumed to be 1,[31] 0, 0.25, 0, and 0 mM, respectively, in the enzyme layer. The diffusion coefficients of Fc, Fc^+, O_2, H_2O_2, and glucose were set as 3×10^{-6}, 3×10^{-6}, 1×10^{-5}, 8×10^{-6}, and 5×10^{-6} $cm^2\ s^{-1}$, respectively. A finite diffusion layer model with a thickness of 0.01 cm was adapted in this simulation. This means that the enzyme layer−solution interface locates at $x = 0.01$ cm, where x is the distance from the electrode surface. No special membrane was considered between the solution and the enzyme layer. The solution concentrations of Fc, Fc^+, O_2, and H_2O_2 were fixed to be 0, 0, 0.25, and 0 mM, respectively, while that of glucose was varied. It has been pointed out that O_2 can be supplied from the pasting liquid of carbon paste electrodes as well as the solution phase.[39] However, an internal supply of O_2 was ignored in the calculation.

The concentration change of each chemical involved in the enzyme reactions in the jth volume element in a certain time interval (Δt) is written as

$$\Delta[Glc](j) = -v_{OX}(j)\Delta t - v_{DH}(j)\Delta t \quad (12)$$

$$\Delta[O_2](j) = -v_{OX}(j)\Delta t \quad (13)$$

$$\Delta[H_2O_2](j) = v_{OX}(j)\Delta t - v_{POx}(j)\Delta t \quad (14)$$

$$\Delta[Fc^+](j) = -2v_{DH}(j)\Delta t + 2v_{POx}(j)\Delta t \quad (15)$$

$$\Delta[Fc](j) = 2v_{DH}(j)\Delta t - 2v_{POx}(j)\Delta t \quad (16)$$

The numerical coefficient (= 2) in eqs 15 and 16 is ascribed to the fact that two equivalent molecules of Fc^+ and Fc are required

(35) Nakamura, S.; Hayashi, S.; Koga, K. *Biochim. Biophys. Acta* **1976**, *445*, 294−308.
(36) Takagi, K.; Yamamoto, K.; Kano, K.; Ikeda, T. *Eur. J. Biochem.* **2001**, *268*, 470−476.
(37) Bartlett, P. N.; Pratt, K. F. E. *J. Electroanal. Chem.* **1995**, *397*, 53−60.
(38) Feldberg, S. W. In *Electroanalytical Chemistry*; Bard, A. J., Ed.; Marcel Dekker: New York, 1969; Vol. 3, pp 199−296.
(39) Wang, J.; Lu, F. *Anal. Chem.* **1998**, *120*, 1048−1050.

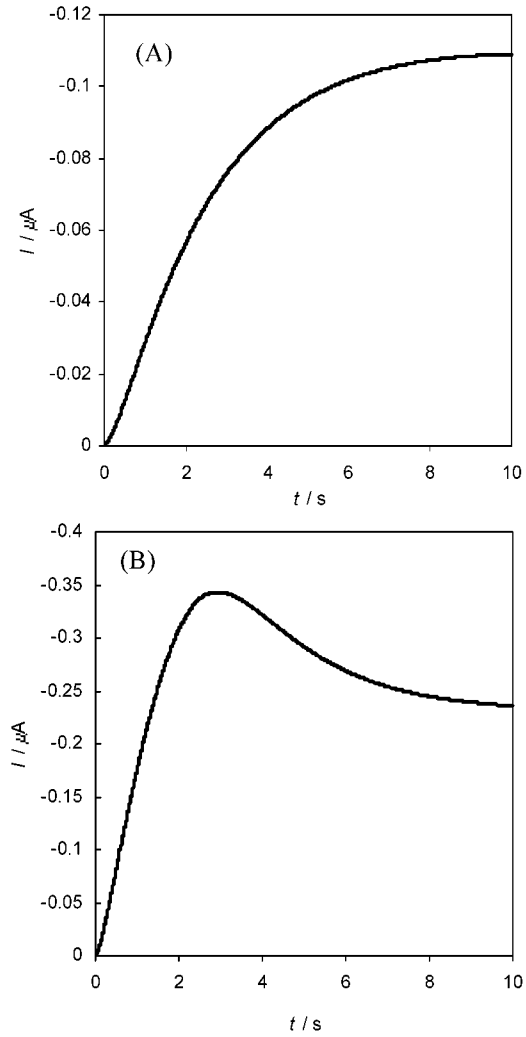

Figure 3. Calculated amperometric response for (A) 0.5 and (B) 5 mM glucose at a model sensor with enzyme activities of $V_{max}^{OX} = 0.90$ M s^{-1} ($V_{max}^{DH} = 0.92$ M s^{-1}) and $V_{max}^{POx} = 0.22$ M s^{-1}.

for the reduction of $POx_{(compound\ I)}$ (eq 2) and the oxidation of $GOx_{(red)}$ (eq 7), respectively. The Fc/Fc^+ redox couple is only electrochemically active. The other treatments are the same as those described in the literature.[40] Although an expanding grid method might be more useful for such a complicated immobilized enzyme electrode system,[27] we utilized a simple explicit point method on Excel (see Supporting Information for details).

Simulated Current−Time Curves and Concentration Profiles. Figure 3 compares simulated current−time curve at low and high concentrations of glucose. The ratio of the parameters V_{max}^{OX} and V_{max}^{POx} used for the calculation was set to be identical with that of the relative activity of GOx and POx in the bienzyme sensor used for Figure 1. The calculated response of the current−time curve appears normal at low glucose concentrations (Figure 3A), while it becomes unusual at increased concentrations of glucose (Figure 3B). This behavior is very similar to that observed experimentally (Figure 1).

Figure 4 shows the concentration profiles of O_2, H_2O_2, and Fc^+. At a low glucose concentration, $[O_2]$ decreases with time, since O_2 is reduced to H_2O_2 by the oxidase reaction of GOx in the enzyme layer (eq 6). The profile reaches a steady state (Figure 4a), since the oxidase reaction rate decreases with decrease in x due to the depletion of glucose. Although the glucose concentration is somewhat larger than the O_2 concentration in solution, a sufficient amount of O_2 remains in the enzyme layer under the steady-state conditions. This is due to the large diffusion coefficient of O_2 compared with glucose.

The H_2O_2 concentration increases with time and then reaches a steady state (Figure 4b), where the rate of the H_2O_2-generating reaction (eq 6) is balanced with that of the H_2O_2-consuming reaction catalyzed by POx (eq 1). As a result, the $[H_2O_2]$ profile has an inverted shape of the $[O_2]$ profile, although $[H_2O_2]$ is lower than the decreased $[O_2]$. Fc^+ is generated by the POx reaction (eq 2) but reduced at the electrode surface. Therefore, the $[Fc^+]$ profile shows a round shape within the enzyme layer with a maximum value around the middle of the layer (Figure 4c). The $[Fc^+]$ versus time profile near the electrode surface is almost identical with the current−time profile (Figure 3A), since the reduction current is directly proportional to the concentration gradient of Fc^+ at the electrode surface. The value of $[Fc^+]$ is sufficiently lower than $[O_2]$ within the enzyme layer. Under such conditions, O_2 is predominantly utilized as an electron acceptor of the GOx reaction, resulting in a normal current response.

In contrast, at higher concentrations of glucose, $[O_2]$ decreases immediately and complete consumption of O_2 occurs on the side of the electrode surface in the enzyme layer (Figure 4d). This is of course due to an increased rate of the oxidase reaction of GOx (eq 6) just after the glucose injection ($t = 0$). In the beginning of the reaction, $[H_2O_2]$ increases quickly, but then it decreases and reaches a steady state (Figure 4e). The decrease in $[H_2O_2]$ is ascribed to the depletion of O_2. Under the steady-state condition, the mass transfer of H_2O_2 generated on the side of the enzyme layer−solution interface is balanced with the consumption of H_2O_2 in the POx reaction.

The $[Fc^+]$ versus x profile given in Figure 4f is similar to that observed at lower concentrations of glucose. However, the $[Fc^+]$ value exceeds $[O_2]$ in the middle portion of the enzyme layer. Therefore, Fc^+ becomes a better (or more available) electron acceptor of reduced GOx than O_2. This causes the decrease in the current response. This situation is responsible for the unusual response of the GOx/POx bienzyme at high glucose concentrations.

Approaches To Overcoming Unusual Response. On the basis of the above discussion, it can be considered that the depletion of O_2 is an important factor in causing the unusual current response. Therefore, it can be expected that bienzyme sensors with increased amounts of GOx are more susceptible to such interference than those with decreased amounts of GOx. Another point governing the response would be the amount of POx. To examine these points, the steady-state current was obtained by simulation as a function of the glucose concentration. Figure 5 shows a calculated calibration curve of a bienzyme sensor with a large amount of GOx ($V_{max}^{OX} = 3.4$) for various values of V_{max}^{POx}. The steady-state current increases with an increase in V_{max}^{POx} at least up to a certain value. However, in all cases investigated, the calibration curves are peak-shaped, and a one-to-one relation was not observed between the current and the glucose concentration. At increased concentrations of glucose, an unusual current−

(40) Battglini, F.; Calvo, E. J. *Anal. Chim. Acta* **1992**, *258*, 151−160.

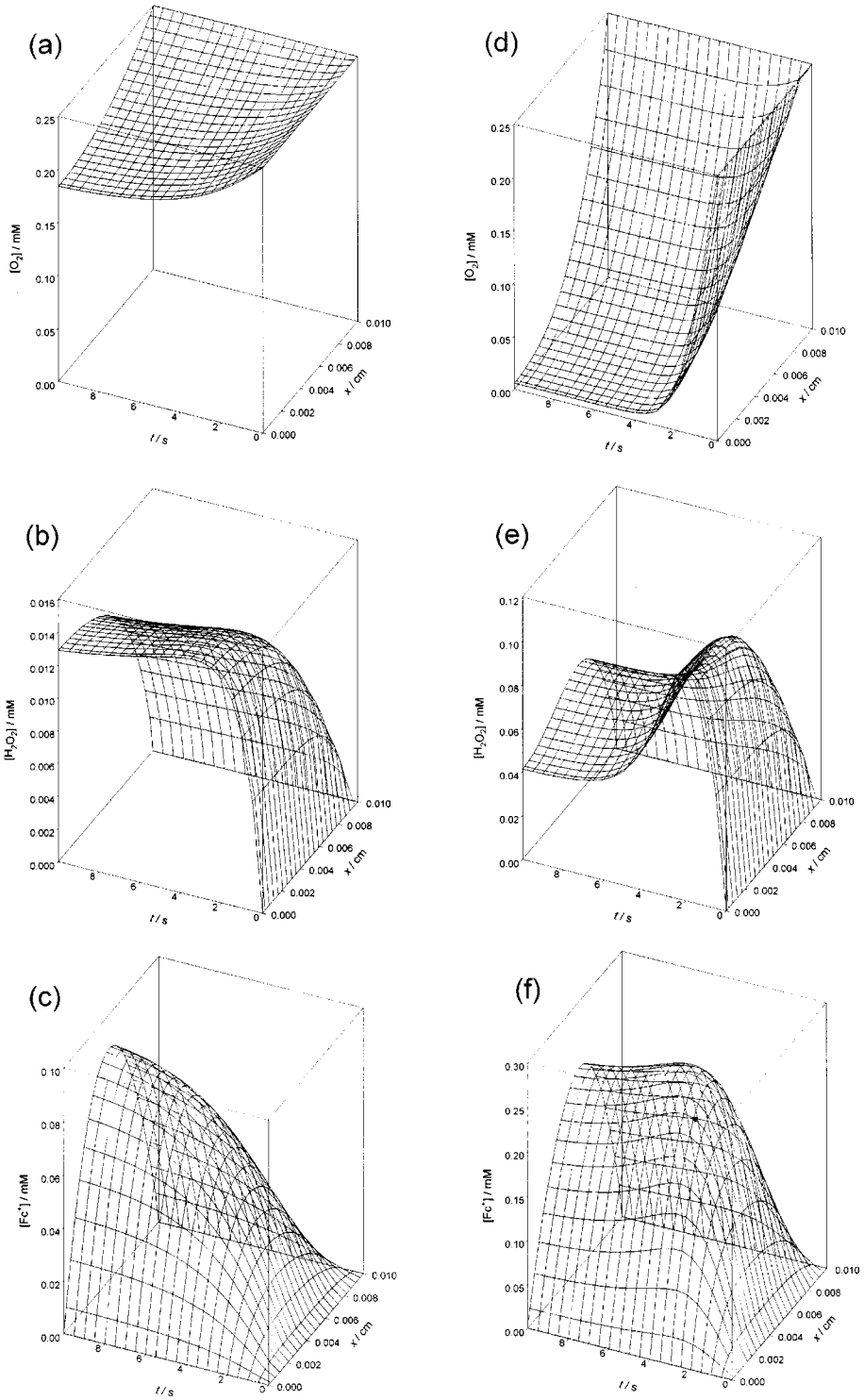

Figure 4. Calculated concentration profiles of (a, d) O_2, (b, e) H_2O_2, and (c, f) Fc^+ for (a−c) 0.5 and (d−f) 5 mM glucose at a model sensor with enzyme activities of V_{max}^{OX}= 0.90 M s^{-1} (V_{max}^{DH} = 0.92 M s^{-1}) and V_{max}^{POx} = 0.22 M s^{-1}. The time axis increases from the right-hand side to the left-hand side.

time response is observed, as shown in Figure 3B. The appearance of such peak-shaped calibration curves and current−time curves is ascribed to the high activity of GOx, which causes the depletion of O_2 within the enzyme layer at increased concentrations of glucose.

In contrast, bienzyme sensors with low amounts of GOx (V_{max}^{OX} = 0.68) exhibit a normal shape in the working curve, as shown in Figure 6A. Under such conditions, complete depletion of O_2 does not occur in the enzyme layer even at increased concentrations of glucose. Because of the low amount of GOx, the rate of H_2O_2 generation decreases, which results in the decrease in Fc^+ generation. Therefore, the oxidase reaction (eq 6) proceeds predominantly over the dehydrogenase reaction (eq 7).

The steady-state current increases with the activity of POx and reaches a maximum value (Figure 6A). This is due to the effective

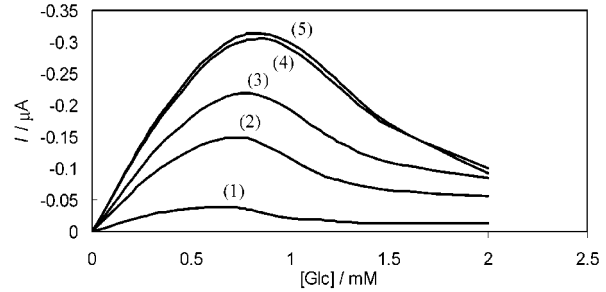

Figure 5. Calculated steady-state current as a function of the glucose concentration at a model sensor with enzyme activities of $V_{max}^{OX} = 3.4$ M s^{-1} ($V_{max}^{DH} = 3.5$ M s^{-1}) and V_{max}^{POx} = (1) 0.01, (2) 0.05, (3) 0.1, (4) 0.5, and (5) 1.0 M s^{-1}.

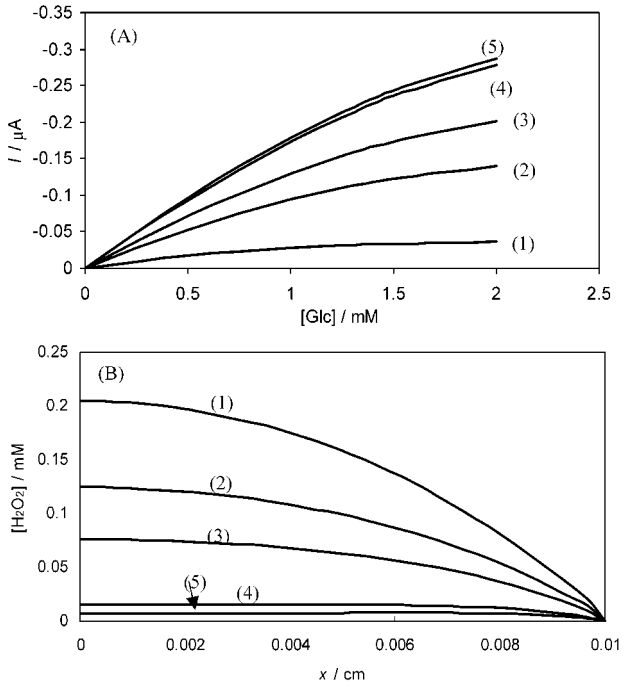

Figure 6. (A) Calculated steady-state current plotted against the glucose concentration and (B) the H_2O_2 concentration profiles at a model sensor with enzyme activities of $V_{max}^{OX} = 0.68$ M s^{-1} ($V_{max}^{DH} = 0.7$ M s^{-1}) and V_{max}^{POx} = (1) 0.01, (2) 0.05, (3) 0.1, (4) 0.5, and (5) 1.0 M s^{-1}.

reduction of H_2O_2 by the POx reaction as shown in Figure 6B, which shows the $[H_2O_2]$ versus x profile under steady-state conditions. With an increase in V_{max}^{POx}, the $[H_2O_2]$ value decreases, and H_2O_2 in the enzyme layer is almost completely reduced at increased activity of V_{max}^{POx}. Therefore, further increase in V_{max}^{POx} does not affect the steady-state current, as judged from the comparison of curve 4 with curve 5 in Figure 6A.

Based on the above discussion, we constructed a bienzyme sensor, which contains a smaller amount of GOx (0.7 unit) and larger amount of POx (1.0 unit) compared with that used for Figure 1 or 2. The sensor exhibited a normal calibration curve. The current−time curves also became normal even at increased concentrations of glucose (data not shown).

In conclusion, oxidase/POx bienzyme mediated biosensors are very useful to construct a variety of sensing devices for biologically related analytes, but they have an inherent drawback of being susceptible to interference due to dehydrogenase activity of the oxidase. The most important factor to cause such an unusual response (or interference) is found to be the depletion of O_2 in the enzyme layer. To overcome the drawback, it is very important to reduce the activity (or amount) of the oxidase, which prevents O_2 depletion in the enzyme layer. Some outer membranes, which show limited permeability against the substrate of the oxidase (glucose in our case), will be also useful (in order to decrease the oxidase reaction).[21,28] Another type of membrane, which can insulate the oxidase reaction from the POx reaction in bienzyme sensors, has been utilized for this purpose.[12] It should be noteworthy that such a short circuit reaction (cross reaction) is not anticipated when the oxidase virtually cannot utilize artificial electron acceptors[12] as in the case of uricase[41] or when a POx-based H_2O_2 sensor works in direct electron-transfer mode without a mediator.[1] In all cases, the increase in POx activity is recommended to reduce H_2O_2 effectively in the enzyme layer, which results in the improvement of the sensitivity.

ACKNOWLEDGMENT

This work was supported in part by Grant-in-Aids for Scientific Research from the Ministry of Education, Science, Sports and Culture of Japan to K.K. and T.I.

SUPPORTING INFORMATION AVAILABLE

Text giving detailed information on a worksheet profile and macro program of Excel used in this work. In this program, the time interval and thickness of the enzyme layer can be changed as for enzyme kinetic parameters. This material is available free of charge via the Internet at http://pubs.acs.org.

Received for review November 12, 2001. Accepted April 30, 2002.

AC015684N

(41) Aoki, M.; Tsujino, Y.; Kano, K.; Ikeda, T. *J. Org. Chem.* **1996**, *61*, 5610−5616.